

Enhancement near the $\bar{p}\Lambda$ threshold in the $\chi_{c0} \rightarrow \bar{p}K^+\Lambda$ reaction

Guan-Ying Wang,¹ Man-Yu Duan,¹ En Wang,^{1,*} and De-Min Li^{1,†}

¹*School of Physics and Microelectronics, Zhengzhou University, Zhengzhou, Henan 450001, China*

We have analyzed the reaction $\chi_{c0} \rightarrow \bar{p}K^+\Lambda$ reported by the BESIII Collaboration, taking into account the contributions from the intermediate $K(1830)$, $N(2300)$, and $\Lambda(1520)$ resonances. Our results are in good agreement with the BESIII measurements, and it is found that the anomalous enhancement near the $\bar{p}\Lambda$ threshold is mainly due to the contribution of the $K(1830)$ resonance. We also show that the interference of the high-mass N^* and Λ^* can not produce the anomalous enhancement near the $\bar{p}\Lambda$ threshold.

PACS numbers:

I. INTRODUCTION

The hadronic decays of the charmonium states could be used to understand the mechanisms of the charmonium decays, and provide a good place to search for the light baryons and mesons, since the charmonium states are the SU(3) singlets, and the final states could provide an isospin filter [1, 2]. For instance, we have studied the reactions of $\chi_{c0} \rightarrow \Sigma\Sigma\pi$ and $\chi_{c0} \rightarrow \bar{\Lambda}\Sigma\pi$, which could be used to search for the baryon state $\Sigma(1430)$ with $J^P = 1/2^-$ and to understand the two poles structure of the $\Lambda(1405)$ resonance [3, 4].

In 2013, an anomalous enhancement near the $\bar{p}\Lambda$ threshold was observed by the BESIII Collaboration in the $\chi_{c0} \rightarrow \bar{p}K^+\Lambda$ process [5]. Assuming the relative angular momentum $L = 0$ between \bar{p} and Λ , the BESIII Collaboration made a fit to the data of the $\bar{p}\Lambda$ mass distribution, and give a state with $M = 2053 \pm 13$ MeV and $\Gamma = 292 \pm 14$ MeV [5]. On the other hand, the similar anomalous enhancements near the $\bar{p}\Lambda$ (or $p\bar{\Lambda}$) threshold were also observed in other processes, such as the $J/\psi \rightarrow pK^-\bar{\Lambda} + c.c.$, $\psi' \rightarrow pK^-\bar{\Lambda} + c.c.$ [6], $B^0 \rightarrow p\bar{\Lambda}\pi^-$ [7], $B^- \rightarrow J/\psi\Lambda\bar{p}$ [8], and $\psi(3680) \rightarrow \gamma\chi_{cJ} \rightarrow \gamma\bar{p}K^{*+}\Lambda + c.c.$ [9].

Most often an enhancement close to the threshold is an indication of the bound state or resonance below threshold [10]. For instance, a peak observed in the $\phi\omega$ threshold in the $J/\psi \rightarrow \gamma\phi\omega$ reaction [11] was interpreted as the manifestation of the $f_0(1710)$ resonance below the $\phi\omega$ threshold [12]. In Ref. [13] the BESIII Collaboration has seen a bump structure close to threshold in the $K^{*0}\bar{K}^{*0}$ mass distribution of the $J/\psi \rightarrow \eta K^{*0}\bar{K}^{*0}$ decay, which can be interpreted as a signal of the formation of an h_1 resonance [12, 14].

The nature of the anomalous enhancement near the $\bar{p}\Lambda$ (or $p\bar{\Lambda}$) threshold is not clear. The anomalous enhancement near the $\bar{p}\Lambda$ threshold may be interpreted as a quasibound dibaryon, or simply as an interference effect of high-mass N^* and Λ^* states, as mentioned by [5]. By investigating the $p\bar{\Lambda}$ systems of $J = 0, 1$ within the chiral quark model and the quark delocalization color screening model, Ref. [15] has shown that there is no S -wave bound state. On the other hand, a preliminary study in the chiral effective field theory of Refs. [16, 17] showed that the S -wave $\bar{p}\Lambda$ interaction is weak and could not generate a bound state [18]. The enhancement near the $\bar{p}\Lambda$ threshold seems unlikely to be a quasibound dibaryon. In addition, the partial wave analysis performed by Ref. [6] has shown that the enhancement near the $p\bar{\Lambda}$ threshold in the $J/\psi \rightarrow pK^-\bar{\Lambda}$ process cannot be due to the high-mass N^* and Λ^* interference effect. One purpose of this work is to check whether the enhancement structure near the $\bar{p}\Lambda$ threshold in the $\chi_{c0} \rightarrow \bar{p}K^+\Lambda$ process can be interpreted as the high-mass N^* and Λ^* interference effect or not. Also, some of the high-mass excited kaon states such as the $K_2(2250)$, $K_3(2320)$, and $K_4(2500)$ have been observed in the $\bar{p}\Lambda$ (or $p\bar{\Lambda}$) mode [19], which implies that the high excited kaons could couple to the $\bar{p}\Lambda$ (or $p\bar{\Lambda}$) channel. One can naturally ask whether the anomalous enhancement near the $\bar{p}\Lambda$ threshold is due to the high-mass excited kaon states or not. We would like to propose that the enhancement near the $\bar{p}\Lambda$ threshold in the $\chi_{c0} \rightarrow \bar{p}K^+\Lambda$ process may be an indication of the excited kaon below the $\bar{p}\Lambda$ threshold. This is another purpose of this work.

Based on the fact that the $\bar{p}K^+$ mass distribution has a clear peak around 1520 MeV associated to the $\Lambda(1520)$ state and the ΛK^+ shows a peak structure around 2200 ~ 2300 MeV associated to the N^* states [5], we will consider the contributions from the intermediate $\Lambda(1520)$ and N^* resonances in the $\chi_{c0} \rightarrow \bar{p}K^+\Lambda$ reaction. In addition, we will consider the contribution from the excited kaons in this reaction.

*Electronic address: wangen@zzu.edu.cn

†Electronic address: lidm@zzu.edu.cn

This paper is organized as follows. In Sec. II, we will present the mechanism for the reaction of $\chi_{c0} \rightarrow \bar{p}K^+\Lambda$, and in Sec. III, we will show our results and discussion. Finally a summary is given in Sec. IV.

II. FORMALISM

In this section, we will present the mechanism for the reaction $\chi_{c0} \rightarrow \bar{p}K^+\Lambda$. In addition to the direct diagram of Fig. 1(a), we take into account the contribution from the intermediate excited kaon (denoted as K^* below), as shown in Fig. 1(b). According to the PDG [19], there are several K^* states close to the $\bar{p}\Lambda$ threshold, such as the $K(1830)$, $K_2(2250)$ and $K_3(2320)$, however, only the $K(1830)$ [$I(J^P) = 1/2(0^-)$] could couple to the $\bar{p}\Lambda$ in S -wave, and the vertex $\chi_{c0}K\bar{K}(1830)$ is also in S -wave. We thus only consider the contribution from the intermediate $K(1830)$ state in present work because the contributions from the higher angular momentum hypotheses are expected to be strongly suppressed near threshold.

From the measurement of the $\chi_{c0} \rightarrow \bar{p}K^+\Lambda$ reaction shown in Fig. 6(a) of Ref. [5], one can find a clear peak around 1520 MeV in the $\bar{p}K^+$ mass distribution, associated to the $\Lambda(1520)$ state, and a broad peak around 2200 ~ 2300 MeV in the ΛK^+ mass distribution, which corresponds to the intermediate N^* states. In this work, we consider the contribution from the $N(2300)$ resonance which could couple to the ΛK^+ in P -wave, as shown in Fig. 1(c), although there are four N^* states in this region [$N(2190)$ ($7/2^-$), $N(2220)$ ($9/2^+$), $N(2250)$ ($9/2^-$), and $N(2300)$ ($1/2^+$)] [19], and also the one from the $\Lambda(1520)$ as shown in Fig. 1(d).

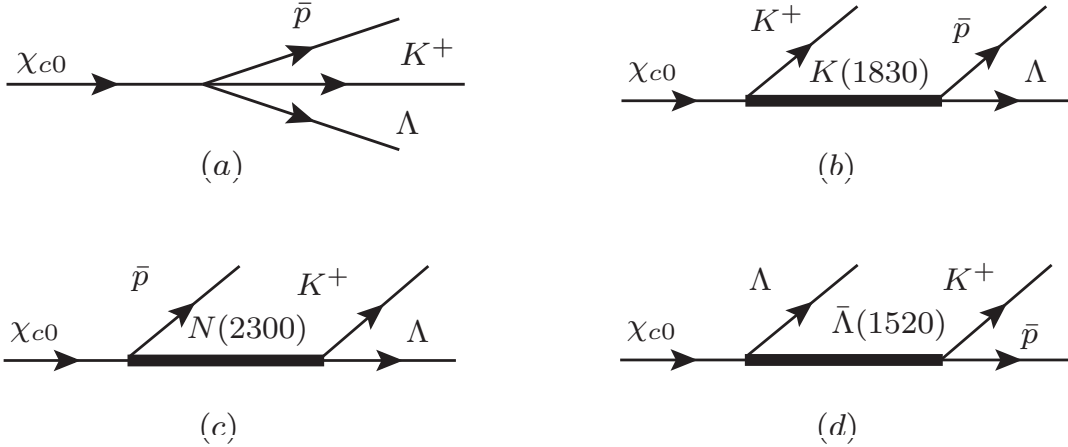


FIG. 1: The diagram for the reaction $\chi_{c0} \rightarrow \bar{p}K^+\Lambda$, (a) the direct diagram, (b) the contribution from the intermediate $K(1830)$ resonance, (c) the contribution from the intermediate $N(2300)$ resonance, and (d) the contribution from the intermediate $\Lambda(1520)$ resonance.

The total amplitude for the $\chi_{c0} \rightarrow \bar{p}K^+\Lambda$ reaction considered in this work can be written as

$$\mathcal{M}^{\text{total}} = \mathcal{M}^{\text{direct}} + \mathcal{M}^{K(1830)} + \mathcal{M}^{N(2300)} + \mathcal{M}^{\Lambda(1520)}, \quad (1)$$

where the $\mathcal{M}^{\text{direct}}$, $\mathcal{M}^{K(1830)}$, $\mathcal{M}^{N(2300)}$, and $\mathcal{M}^{\Lambda(1520)}$ are the amplitudes from the direct diagram, $K(1830)$, $N(2300)$, and $\Lambda(1520)$, respectively.

The amplitude of the direct diagram and the $K(1830)$ term can be expressed as

$$\begin{aligned} \mathcal{M} &= \mathcal{M}^{\text{direct}} + \mathcal{M}^{K(1830)} \\ &= V_p \left[1 + \frac{\alpha M_N^2}{M_{\bar{p}\Lambda}^2 - M_{K^*}^2 + iM_{K^*}\Gamma_{K^*}} \right], \end{aligned} \quad (2)$$

where V_p is an unknown normalization factor, α is the weight of the contribution from the intermediate $K(1830)$ state with a mass of M_{K^*} and a width of Γ_{K^*} , M_N is the average mass of the nucleons, and $M_{\bar{p}\Lambda}$ is the invariant mass of $\bar{p}\Lambda$ system. The parameter α is dimensionless because we have included the M_N^2 in the numerator of Eq. (2).

The amplitude for the intermediate $N(2300)$ term is

$$\mathcal{M}^{N(2300)} = \frac{\beta/M_N}{M_{\Lambda K^+} - M_{N(2300)} + i\Gamma_{N(2300)}/2} \times \langle m_{\bar{p}} | \vec{\sigma} \cdot \vec{p}_p | m_{N(2300)} \rangle \langle m_{N(2300)} | \vec{\sigma} \cdot \vec{p}_\Lambda | m_\Lambda \rangle, \quad (3)$$

where β is the weight of the contribution from the intermediate $N(2300)$ state with a mass of $M_{N(2300)}$ and a width of $\Gamma_{N(2300)}$, $M_{\Lambda K^+}$ is the invariant mass of ΛK^+ system, $\vec{\sigma}$ is the Pauli matrix, m_R denotes the polarization index of state R , and we will sum over the polarizations of the $N(2300)$, \bar{p} , and Λ . \vec{p}_p and \vec{p}_Λ are the three momenta of the \bar{p} and Λ in the χ_{c0} and $K^+\Lambda$ rest frames, respectively.

The amplitude for the intermediate $\Lambda(1520)$ is

$$\mathcal{M}^{\Lambda(1520)} = \frac{\beta'/M_{\Lambda(1520)}^3 \times D_{\frac{3}{2}-} \times D'_{\frac{3}{2}-}}{M_{\bar{p}K^+} - M_{\Lambda(1520)} + i\Gamma_{\Lambda(1520)}/2} \quad (4)$$

with the term $D_{\frac{3}{2}-}$ for $\bar{\Lambda}(1520) \rightarrow \bar{p}K^+$ vertex

$$D_{\frac{3}{2}-} = \left\langle m_{\bar{p}} \left| \left[(\tilde{k}_K)_i (\tilde{k}_K)_j - \frac{1}{3} \tilde{k}_K^2 \delta_{ij} \right] \sigma_i \sigma_j \right| m_{\bar{\Lambda}(1520)} \right\rangle, \quad (5)$$

and the term $D'_{\frac{3}{2}-}$ for $\chi_{c0} \rightarrow \Lambda \bar{\Lambda}(1520)$ vertex

$$D'_{\frac{3}{2}-} = \left\langle m_{\bar{\Lambda}(1520)} \left| \left[(\tilde{p}_\Lambda)_i (\tilde{p}_\Lambda)_j - \frac{1}{3} \tilde{p}_\Lambda^2 \delta_{ij} \right] \sigma_i \sigma_j \right| m_\Lambda \right\rangle, \quad (6)$$

where β' corresponds to the weight of the contribution from the intermediate $\Lambda(1520)$ resonance with a mass of $M_{\Lambda(1520)}$ and a width of $\Gamma_{\Lambda(1520)}$, $M_{\bar{p}K^+}$ is the invariant mass of $\bar{p}K^+$ system, and \tilde{k}_K and \tilde{p}_Λ are the three momenta of K^+ and Λ in the $\bar{p}K^+$ and χ_{c0} rest frames, respectively.

Finally, the invariant mass distributions of $\chi_{c0} \rightarrow \bar{p}K^+\Lambda$ read

$$\frac{d\Gamma}{dM_{\bar{p}K^+}^2 dM_{\bar{p}\Lambda}^2} = \frac{1}{(2\pi)^3} \frac{4M_{\bar{p}}M_\Lambda}{32M_{\chi_{c0}}^3} |\mathcal{M}^{\text{total}}|^2, \quad (7)$$

$$\frac{d\Gamma}{dM_{\Lambda K^+}^2 dM_{\bar{p}\Lambda}^2} = \frac{1}{(2\pi)^3} \frac{4M_{\bar{p}}M_\Lambda}{32M_{\chi_{c0}}^3} |\mathcal{M}^{\text{total}}|^2, \quad (8)$$

where $M_{\bar{p}}$, M_Λ , and $M_{\chi_{c0}}$ are the masses of \bar{p} , Λ , and χ_{c0} , respectively. Since there is no interference between the different partial waves, the $|\mathcal{M}|^2$ in Eqs. (7) and (8) can be substituted by

$$|\mathcal{M}^{\text{total}}|^2 = V_p^2 \left| 1 + \frac{\alpha M_N^2}{M_{\bar{p}\Lambda}^2 - M_{K^*}^2 + iM_{K^*}\Gamma_{K^*}} \right|^2 + V_p^2 \left| \frac{\beta \tilde{p}_\Lambda \vec{p}_p / M_N}{M_{\Lambda K^+} - M_{N(2300)} + i\Gamma_{N(2300)}/2} \right|^2 + V_p^2 \left| \frac{\tilde{k}_K^4 |\vec{p}_\Lambda|^4}{M_{\Lambda(1520)}^6} \frac{\beta'}{M_{\bar{p}K^+} - M_{\Lambda(1520)} + i\Gamma_{\Lambda(1520)}/2} \right|^2. \quad (9)$$

The $\bar{p}K^+$ and ΛK^+ mass distributions can be obtained by integrating $M_{\bar{p}\Lambda}$ in Eqs. (7) and (8) respectively, and the $\bar{p}\Lambda$ mass distributions can be obtained by integrating $M_{\bar{p}K^+}$ in Eq. (7). For a given value of M_{12}^2 , the range of M_{23}^2 is defined as

$$(M_{23})_{\text{max}} = (E_2^* + E_3)^2 - \left(\sqrt{E_2^{*2} - M_2^2} - \sqrt{E_3^{*2} - M_3^2} \right)^2, \\ (M_{23})_{\text{min}} = (E_2^* + E_3)^2 - \left(\sqrt{E_2^{*2} - M_2^2} + \sqrt{E_3^{*2} - M_3^2} \right)^2, \quad (10)$$

where E_2^* and E_3^* are the energies of particles 2 and 3 in the rest frame of particles 1 and 2, respectively, and M_1 and M_2 are the masses of particles 1 and 2, respectively. The masses and widths of the baryons and mesons except for $N(2300)$ involved in this work are taken from PDG [19]. For the $N(2300)$, we don't take the measured mass and width due to the larger uncertainties, and take $M_{N(2300)}$ and $\Gamma_{N(2300)}$ as free parameters.

TABLE I: The model parameters obtained by fitting to the BESIII measurements [5].

Parameter	α	β	β'	$M_{N(2300)}$	$\Gamma_{N(2300)}$	V_p	V'_p
value	104.0	45.6	6.8	2354.6	252.0	0.010	0.022
error	2.1	3.2	0.5	18.5	3.3	0.001	0.001

III. RESULTS AND DISCUSSIONS

With the above formalism, we will fit our model to the $\bar{p}K^+$, ΛK^+ , and $\bar{p}\Lambda$ mass distributions of the events reported by the Belle Collaboration [5]. It should be pointed out that the $\bar{p}K^+$ and ΛK^+ mass distributions are not corrected by the detector efficiency¹, but the $\bar{p}\Lambda$ mass distribution is given with the acceptance correction. In order to directly compare our results with the BESIII measurement, we take two different normalization factors in our fit, V_p for the $\bar{p}K^+/\Lambda K^+$ mass distribution and V'_p for the $\bar{p}\Lambda$ mass distribution. There are seven model parameters, 1) α , the weight of the contribution from the intermediate $K(1830)$ state, 2) β , the weight of the contribution from the intermediate $N(2300)$ state, 3) β' , the weight of the intermediate $\Lambda(1520)$ state, 4) the mass and width of the $N(2300)$ state, 5) the unknown normalization factor V_p for the $\bar{p}K^+/\Lambda K^+$ invariant mass distribution, and 6) the unknown normalization factor V'_p for the $\bar{p}\Lambda$ invariant mass distribution.

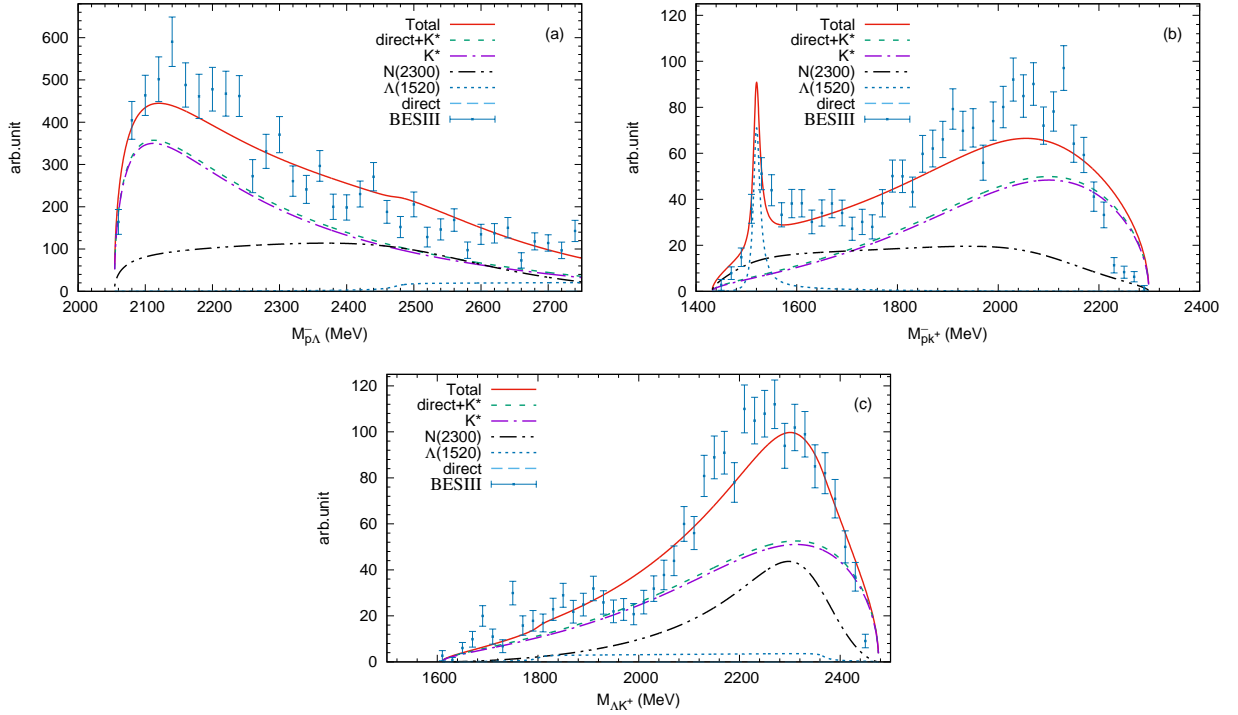


FIG. 2: The $\bar{p}\Lambda$ (a), $\bar{p}K^+$ (b), and ΛK^+ (c) mass distributions for the reaction $\chi_{c0} \rightarrow \bar{p}K^+\Lambda$. The curves labeled as ‘direct’, ‘ K^* ’, ‘ $N(2300)$ ’, and ‘ $\Lambda(1520)$ ’ show the contributions of Figs. 1(a), (b), (c), and (d), respectively, and the curves labeled as ‘direct+ K^* ’ are the contributions of the direct term and the intermediate $K(1830)$ state in Eq. (2). The ‘total’ curves correspond to the total contribution of Eq. (1). The BESIII data are taken from Ref. [5].

With the model presented above, we make a fit to the BESIII measurements, including the $\bar{p}\Lambda$, $\bar{p}K^+$, and ΛK^+ mass distributions [5]. The $\chi^2/d.o.f$ is $393.7/(115 - 7) = 3.6$, and the fitted parameters are tabulated in Table I,

¹ The data of the $\bar{p}K^+$ and ΛK^+ mass distributions are not corrected by the detector efficiency. We have communicated with Wen-Biao Yan and Cong Geng, the two of authors of Ref. [5]. The curves of the detector efficiency for $\bar{p}K^+$ and ΛK^+ approximate to be flat, and there is no fine structure in the efficiency distributions.

where both the fitted mass and width of $N(2300)$ are consistent with the PDG values [19] within errors. With the fitted values of the parameters, we calculate the $\bar{p}\Lambda$, $\bar{p}K^+$, and ΛK^+ mass distributions, and compare our results with the BESIII measurements [5], as shown in Fig. 2. One can see that our results are in good agreement with the BESIII data, especially in the $\bar{p}\Lambda$ mass distribution the anomalous enhancement near the $\bar{p}\Lambda$ threshold can be well reproduced. The $K(1830)$ plays an important role for the anomalous enhancement. In addition, Fig. 2(c) shows that the peak around 2200 ~ 2300 MeV in the ΛK^+ mass distribution could mainly result from the $N(2300)$.



FIG. 3: The diagram for the contribution from the intermediate high-mass Λ^* resonance.

Ref. [5] has mentioned that the enhancement structure near the $\bar{p}\Lambda$ threshold could simply be explained as an interference effect of high-mass N^* and Λ^* . In order to check this hypothesis, in addition to the direct diagram contribution, we will only take into account the contributions from the $N(2300)$ and the excited Λ resonances Λ^* 's. Although there are two states around 2000 MeV, $\Lambda(2100)$ ($7/2^-$) and $\Lambda(2110)$ ($5/2^+$) [19], their contributions are expected to be strongly suppressed since both of them couple to the $\bar{p}K^+$ in F -wave. Several Λ^* ($1/2^-$) with masses around 2100 MeV have been predicted by the quark model [20]. For simplicity, we take into account the contribution from one Λ^* ($1/2^-$) which couples to the $\bar{p}K^+$ in S -wave², as shown in Fig. 3. The corresponding amplitude can be expressed as,

$$\mathcal{M}^{\Lambda^*} = \frac{V_p \alpha' M_N}{M_{\bar{p}K^+} - M_{\Lambda^*} + i\Gamma_{\Lambda^*}/2}, \quad (11)$$

where α' is the weight of the contribution from the intermediate Λ^* resonance with a mass of M_{Λ^*} and a width of Γ_{Λ^*} . The full amplitude can be rewritten as,

$$(\mathcal{M}')^{\text{total}} = \mathcal{M}^{\text{direct}} + \mathcal{M}^{N(2300)} + \mathcal{M}^{\Lambda^*}. \quad (12)$$

In this case, we have eight parameters, 1) α' , the weight of the contribution from the intermediate Λ^* resonance, 2) β , the weight of the contribution from the intermediate $N(2300)$, 3) the mass and the width of the Λ^* , 4) the mass and width of the $N(2300)$, 5) two unknown normalization factors V_p and V_p' . With the amplitude of Eq. (12), we make a fit to the BESIII data [5], and find $\chi^2/d.o.f = 5.54$, which is larger than that of the above case. The fitted parameters are tabulated in Table II. We also present the $\bar{p}\Lambda$, $\bar{p}K^+$, and ΛK^+ mass distributions in Fig. 4. Although the $\bar{p}K^+$ and ΛK^+ mass distributions can be well reproduced, the anomalous enhancement near the $\bar{p}\Lambda$ threshold is not found in the $\bar{p}\Lambda$ mass distribution. This can be explained by the Dalitz plots of the $\chi_{c0} \rightarrow \bar{p}\Lambda K^+$ as shown in Fig. 5. It shows that the high mass N^* and Λ^* give the contributions in the energy regions of 2100 ~ 2600 MeV of the $\bar{p}\Lambda$ mass distribution, not only in the energy regions near the $\bar{p}\Lambda$ threshold, which is in agreement with Fig. 4(a) (see the curves labeled as ' $N(2300)$ ' and ' Λ^* '). Based on the partial wave analysis, the BESIII Collaboration has also concluded that the enhancement in the $J/\psi \rightarrow \bar{p}\Lambda K^+ + c.c.$ cannot be due to the interference effects between high-mass N^* 's and Λ^* 's [6]

TABLE II: The model parameters obtained by fitting to the BESIII measurements [5], taking into account the interference of $N(2300)$ and $\Lambda^*(1/2)$.

Parameter	α'	β	V_p	V_p'	M_{Λ^*}	Γ_{Λ^*}	$M_{N(2300)}$	$\Gamma_{N(2300)}$
value	1.16	17.1	0.046	0.093	2085.1	183.2	2402.1	252.0
error	0.13	1.4	0.004	0.008	8.9	20.1	12.2	2.3

² Indeed, if several Λ^* 's with $J^P = 1/2^-$ around 2100 MeV are taken into account, the contributions can be described with the Breit-Wigner form of one Λ^* , by adjusting its mass and width.

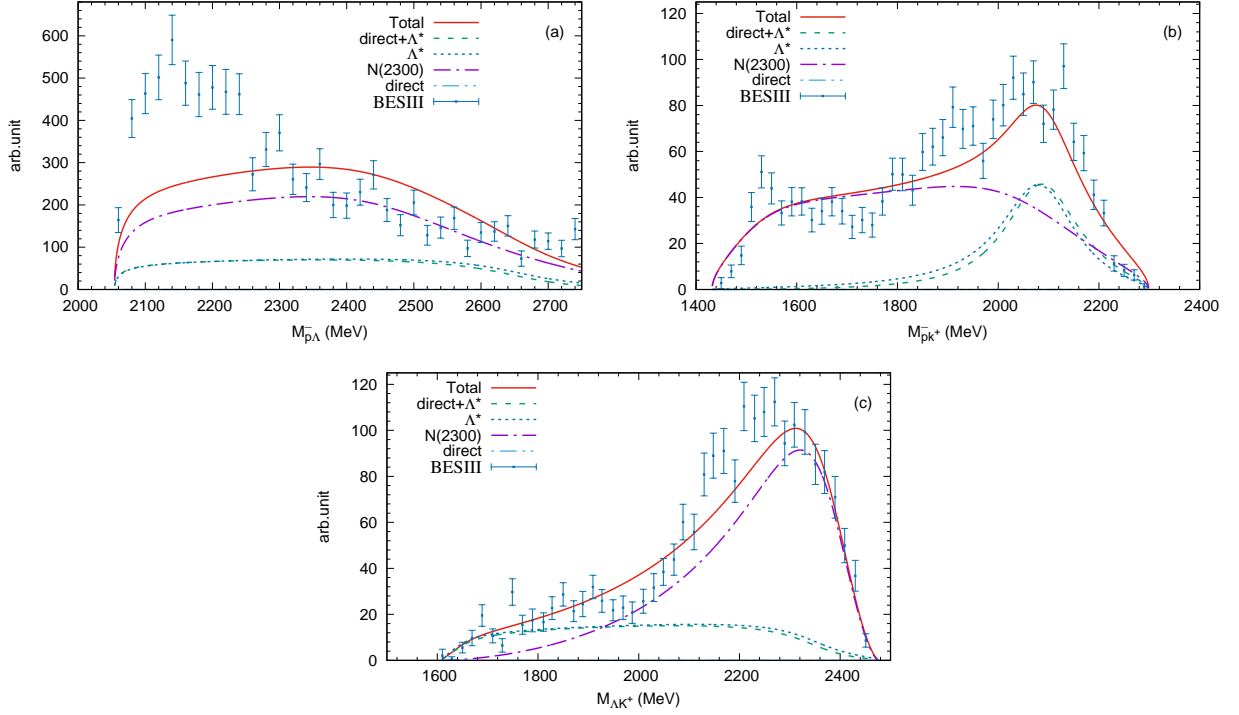


FIG. 4: The $\bar{p}\Lambda$ (a), $\bar{p}K^+$ (b), and ΛK^+ (c) mass distributions including the $N(2300)$ and high mass Λ state. The curves labeled as ‘direct’, ‘ $N(2300)$ ’, and ‘ Λ^* ’ show the contributions of the Figs. 1(a), (c), and Fig. 3, respectively, and the curves labeled as ‘direct+ Λ^* ’ are the contribution of the direct term and the intermediate Λ^* state,. The ‘total’ curves correspond to the total contribution of Eq. (12). The BESIII data are taken from Ref. [5].

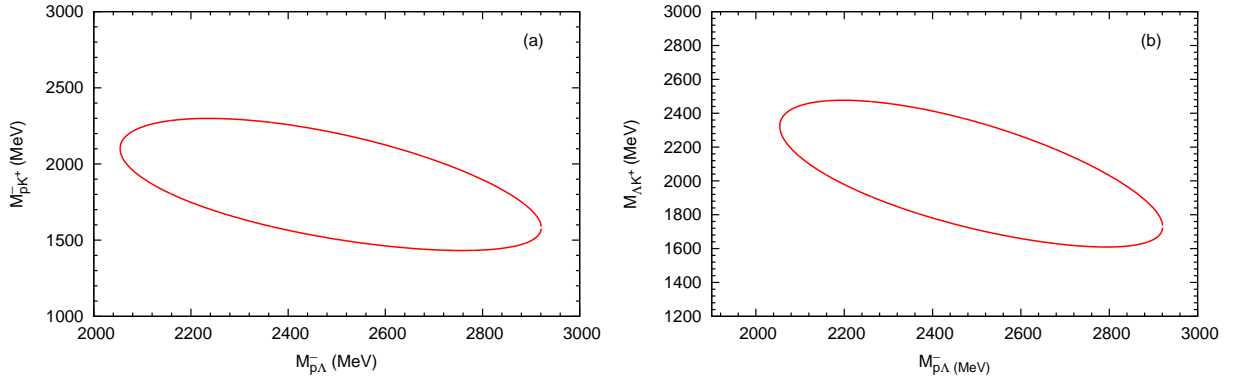


FIG. 5: The Dalitz plots for the $\chi_{c0} \rightarrow \bar{p}K^+\Lambda$

Finally, in Fig. 6, we show that the results for $|\mathcal{M}|^2$ extracted from the BESIII data [5], dividing the measured $\bar{p}\Lambda$ mass distribution by the phase space factor of Eq. (7). One can see that the peak should be below the $\bar{p}\Lambda$ threshold if the first point of Fig. 6 is neglected because of the limited statistics. Thus, if the anomalous enhancements near the $\bar{p}\Lambda$ threshold in the processes $\chi_{c0} \rightarrow \bar{p}K^+\Lambda$ [5], $J/\psi \rightarrow pK^-\bar{\Lambda} + c.c.$, $\psi' \rightarrow pK^-\bar{\Lambda} + c.c.$ [6], and $B^0 \rightarrow p\bar{\Lambda}\pi^-$ [7] are due to the K^* resonance, there will be a peak structure around 1900 MeV in the $K\pi$, $K\pi\pi$, $K\phi$ modes of the processes $\chi_{c0}, J/\psi, \psi' \rightarrow KK\pi, KK\pi\pi, KK\phi$. Searching for the structure in those processes would be helpful to understand the anomalous enhancements near the $\bar{p}\Lambda$ threshold.

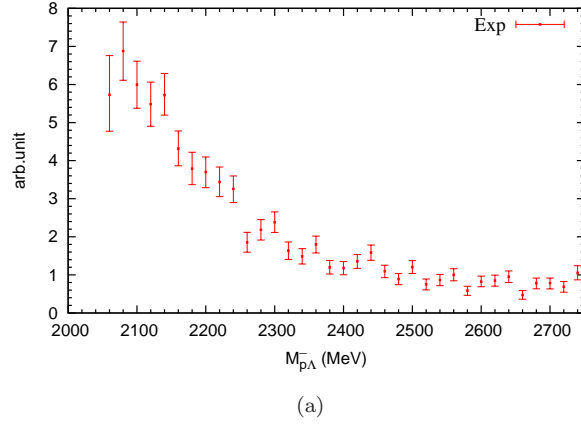


FIG. 6: Data for $d\Gamma/dM_{\bar{p}\Lambda}$ divided by the phase space of Eq. (7).

IV. SUMMARY

In this work, we have analyzed the anomalous enhancement near the $\bar{p}\Lambda$ threshold in the $\chi_{c0} \rightarrow \bar{p}K^+\Lambda$ reaction measured by the BESIII collaboration [5]. Our results for the $\bar{p}\Lambda$, $\bar{p}K^+$, and ΛK^+ mass distributions are in good agreement with the BESIII measurement [5]. We find that the anomalous enhancement near the $\bar{p}\Lambda$ threshold is mainly due to the contribution of the $K(1830)$. We have also shown that interference of the high-mass N^* and Λ^* can not reproduce the anomalous enhancement near the $\bar{p}\Lambda$ threshold.

We suggest to confirm the peak structure around 1900 MeV in the $K\pi$, $K\pi\pi$, and $K\phi$ modes of the processes $\chi_{c0}, J/\psi, \psi' \rightarrow KK\pi, KK\pi\pi, KK\phi$, which will help to understand the anomalous enhancement near the $\bar{p}\Lambda$ threshold.

Acknowledgements

We would like to acknowledge the fruitful discussions with Eulogio Oset, Ju-Jun Xie, and Li-Sheng Geng. This work is partly supported by the National Natural Science Foundation of China under Grant Nos. 11505158, 11605158, the Key Research Projects of Henan Higher Education Institutions (No. 20A140027), and the Academic Improvement Project of Zhengzhou University.

-
- [1] E. Klempt and A. Zaitsev, Glueballs, Hybrids, Multiquarks. Experimental facts versus QCD inspired concepts, Phys. Rept. **454**, 1 (2007).
 - [2] B. S. Zou, N^* , Λ^* , Σ^* and Ξ^* resonances from J/ψ and ψ' decays, Nucl. Phys. A **684**, 330 (2001).
 - [3] E. Wang, J. J. Xie and E. Oset, $\chi_{c0}(1P)$ decay into $\bar{\Sigma}\Sigma\pi$ in search of an $I = 1, 1/2^-$ baryon state around $\bar{K}N$ threshold, Phys. Lett. B **753**, 526 (2016).
 - [4] L. J. Liu, E. Wang, J. J. Xie, K. L. Song and J. Y. Zhu, $\Lambda(1405)$ production in the process $\chi_{c0}(1P) \rightarrow \bar{\Lambda}\Sigma\pi$, Phys. Rev. D **98**, no. 11, 114017 (2018).
 - [5] M. Ablikim *et al.* [BESIII Collaboration], Measurements of $\psi' \rightarrow \bar{p}K^+\Sigma^0$ and $\chi_{cJ} \rightarrow \bar{p}K^+\Lambda$, Phys. Rev. D **87**, no. 1, 012007 (2013).
 - [6] M. Ablikim *et al.* [BES Collaboration], Observation of a threshold enhancement in the p anti-Lambda invariant mass spectrum, Phys. Rev. Lett. **93**, 112002 (2004).
 - [7] M. Z. Wang *et al.* [Belle Collaboration], Observation of $B^0 \rightarrow p\bar{\Lambda}\pi^-$, Phys. Rev. Lett. **90**, 201802 (2003).
 - [8] Q. L. Xie *et al.* [Belle Collaboration], Observation of $B^- \rightarrow J/\psi\Lambda\bar{p}$ and searches for $B^- \rightarrow J/\psi\Sigma^0\bar{p}$ and $B^0 \rightarrow J/\psi p\bar{p}$ decays, Phys. Rev. D **72**, 051105 (2005).
 - [9] M. Ablikim *et al.* [BESIII Collaboration], Study of the decays $\psi(3686) \rightarrow \gamma\chi_{cJ} \rightarrow \gamma\bar{p}K^{*+}\Lambda + c.c.$ and $\psi(3686) \rightarrow \bar{p}K^{*+}\Lambda + c.c.$, Phys. Rev. D **100**, no. 5, 052010 (2019).
 - [10] F. Aceti, M. Bayar, J. M. Dias and E. Oset, Prediction of a $Z_c(4000) D^*\bar{D}^*$ state and relationship to the claimed $Z_c(4025)$, Eur. Phys. J. A **50**, 103 (2014).
 - [11] M. Ablikim *et al.* [BES Collaboration], Observation of a near-threshold enhancement in the omega phi mass spectrum from the doubly OZI suppressed decay $J/\psi \rightarrow \gamma\omega\phi$, Phys. Rev. Lett. **96**, 162002 (2006).

- [12] L. S. Geng and E. Oset, Vector meson-vector meson interaction in a hidden gauge unitary approach, Phys. Rev. D **79**, 074009 (2009).
- [13] M. Ablikim *et al.* [BES Collaboration], Study of J/Psi decays into eta K*0 anti-K*0, Phys. Lett. B **685**, 27 (2010).
- [14] J. J. Xie, M. Albaladejo and E. Oset, Signature of an h_1 state in the $J/\psi \rightarrow \eta h_1 \rightarrow \eta K^{*0} \bar{K}^{*0}$ decay, Phys. Lett. B **728**, 319 (2014).
- [15] H. Huang, J. Ping and F. Wang, Study of $p\bar{\Lambda}$ and $p\bar{\Sigma}$ systems in constituent quark models, Mod. Phys. Lett. A **27**, 1250039 (2012).
- [16] K. W. Li, X. L. Ren, L. S. Geng and B. W. Long, Leading order relativistic hyperon-nucleon interactions in chiral effective field theory, Chin. Phys. C **42**, no. 1, 014105 (2018).
- [17] J. Song, K. W. Li and L. S. Geng, Strangeness $S = ?$ hyperon-nucleon interactions: Chiral effective field theory versus lattice QCD, Phys. Rev. C **97**, no. 6, 065201 (2018).
- [18] Jing Song, Kai-Wen Li, and Li-Sheng Geng, in preparation.
- [19] M. Tanabashi *et al.* [Particle Data Group], Review of Particle Physics, Phys. Rev. D **98**, no. 3, 030001 (2018).
- [20] S. Capstick and N. Isgur, Baryons in a Relativized Quark Model with Chromodynamics, Phys. Rev. D **34**, 2809 (1986).